BIOCHEMISTRY
including biophysical chemistry & molecular biology

Article

pubs.acs.org/biochemistry

Molecular Mechanism of Photozipper, a Light-Regulated Dimerizing Module Consisting of the bZIP and LOV Domains of Aureochrome-1

Yoichi Nakatani and Osamu Hisatomi*

Department of Earth and Space Science, Graduate School of Science, Osaka University, Toyonaka, Osaka 560-0043, Japan

Supporting Information

ABSTRACT: Aureochrome-1 (AUREO1) is a blue light (BL) receptor responsible for the BL-induced blanching of a stramenopile alga, *Vaucheria frigida*. The AUREO1 protein contains a central basic region/leucine zipper (bZIP) domain, and a C-terminal light-oxygen-voltage-sensing (LOV) domain. BL induces the dimerization of monomeric AUREO1, which subsequently increases the affinity of this transcription factor for its target DNA [Hisatomi, O., et al. (2014) *J. Biol. Chem. 289*, 17379−17391]. We constructed a synthetic gene encoding N-terminally truncated monomeric AUREO1 (designated Photozipper) to elucidate the molecular mechanism of this BL-regulated transcription factor and to develop it as an optogenetic tool. In this study, four different Photozipper (PZ) protein constructs were prepared comprising different N-terminal truncations. The monomer−dimer equilibria of the PZ constructs were investigated in the dark and light states. Dynamic light scattering and size-exclusion chromatography analyses revealed that the apparent dissociation constants of PZ dimers with and without the ZIP region were ∼100 and 30 μM, respectively, indicating that the ZIP region stabilized the monomeric form in the dark state. In the light state, fluorescence resonance energy transfer analyses demonstrated that deletion of the ZIP region increased the dissociation constant from ∼0.15 to 0.6 μM, suggesting that intermolecular LOV−LOV and ZIP−ZIP interactions stabilized the dimeric forms. Our results suggest that synergistic interactions between the LOV and bZIP domains stabilize the monomeric form in the dark state and the dimeric form in the light state, which possibly contributes to the function of PZ as a BL-regulated molecular switch.

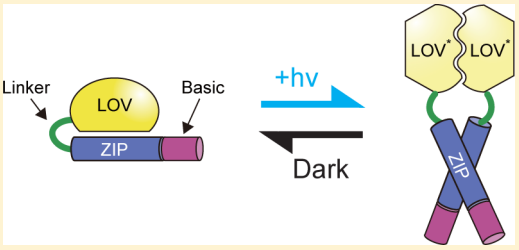

Protein−protein interactions play crucial roles in signal transduction within the cell. Per-ARNT-Sim (PAS) domains are found in many signaling proteins in fungi, plants, insects, and vertebrates. PAS domains bind endogenous or xenobiotic small molecules and sense light, oxygen, redox potential, and other stimuli.[1] The light-oxygen-voltage-sensing (LOV) domain that belongs to the PAS domain superfamily was originally identified as the blue light (BL) receptor in phototropin (phot) of plants.[2] The LOV domain possesses a noncovalently bound flavin mononucleotide (FMN) as a chromophore. Upon photoactivation, FMN forms a covalent adduct with a highly conserved cysteine residue in the LOV domain.[3−5] This photochemical reaction induces conformational changes within the LOV domain, thereby influencing its intramolecular interactions with effecter domains on the same proteins and/or its intermolecular interactions with other proteins.

Phototoropin has a kinase domain at the C-terminus and two LOV domains (LOV1 and LOV2) at the N-terminus.[2] The LOV2 domain of phot plays an important role in regulating the Ser/Thr protein kinase domain.[6] Upon BL illumination, an α-helix (Jα) located at the C-terminal LOV core dissociates from the β-sheet surface of LOV2 and unfolds, leading to activation of the kinase domain.[7−12] The LOV photoreceptor from *Bacillus subtilis*, YtvA, is a stable dimer with two Jα helices forming quasi-coiled-coil interactions. The conformational changes in the LOV domain cause twisting of these coiled-coil helices, subsequently activating the effector domain.[13,14] Vivid from the *Neurospora crasa* has an N-terminal cap (Ncap) comprising an α-helix (aα), a β-sheet (bβ), and a short hinge, which docks onto the β-sheet of the LOV core.[15] BL excitation induces a rearrangement of the Ncap, which leads to the transient homodimerization of Vivid.[16,17] Marine bacterial LOV protein EL222 exists as a monomer with a helix−turn−helix (HTH) domain that docks onto the β-sheet of the LOV domain in the dark.[18] Light-induced conformational changes in the LOV domain disrupt these contacts, leading to the formation of a dimer on the target DNA.[18,19] These light-induced changes of the LOV domains have recently been applied in the development of optogenetic tools for controlling intracellular signal transduction, as well as cellular activities and organization.[20−23]

Aureochrome (AUREO) was first observed as a BL receptor in a stramenopile alga, *Vaucheria frigida*.[24] Its two homologues, named aureochrome-1 (AUREO1) and aureochrome-2 (AUREO2), were reported to play roles in BL-induced branching and the development of sex organs, respectively.[24] AUREO orthologs have been found only in photosynthetic stramenopiles such as brown algae, some diatoms, *Ochromonas*, *Chattonella*, and *Aureococcus*.[25] AUREOs contain a LOV domain in the C-terminal region and a basic region/leucine zipper (bZIP) domain on the N-terminal side of the LOV domain. The bZIP domain is an α-helical DNA-binding motif found among eukaryotic transcription factors.[26] Recombinant AUREO1 binds the TGACGT target

Received: March 25, 2015
Revised: April 30, 2015
Published: May 1, 2015

DOI: 10.1021/acs.biochem.5b00320
Biochemistry 2015, 54, 3302−3313

sequence in a light-dependent manner, implying that the AUREO proteins function as BL-regulated transcription factors.[24]

Using the transient grating (TG) technique and size-exclusion chromatography (SEC), Toyooka et al. reported that AUREO1-LOV from *V. frigida* exists in a monomer−dimer equilibrium in the dark and dimerizes upon photoexcitation.[27] BL appeared to reduce the α-helical content of the LOV domain, judging from the circular dichroism (CD) spectroscopy data.[28] N-Terminally truncated AUREO1 ($ZLwt_2$), consisting of the bZIP and LOV domains only, was still observed to form a dimer through intermolecular disulfide linkages at Cys^{162} and Cys^{182} with a midpoint oxidation redox potential (ORP) of approximately -245 ± 15 mV.[29] Dynamic light scattering (DLS) and SEC analyses showed that dithiothreitol (DTT)-treated $ZLwt_2$ and a site-directed ZL mutant (ZLC_2S) in which Cys^{162} and Cys^{182} were substituted with Ser were both monomeric in the dark. On the other hand, BL induced the dimerization of monomeric AUREO1s, which subsequently increased their affinity for the target sequence.[29] However, quantitative analyses of dimer formation and DNA binding of AUREO1 remain to be performed.

In this study, we synthesized a gene (opZL) encoding the ZLC_2S mutant with a histidine hexamer at the C-terminus (designated in this study as the Photozipper protein) and investigated the monomer−dimer equilibria of four truncated forms of Photozipper (PZ) protein in the dark and light states, using spectroscopic, DLS, SEC, and fluorescence resonance energy transfer (FRET) analyses. Our results suggested that synergistic interactions between the LOV and bZIP domains stabilize the monomeric form in the dark state and the dimeric form in the light state, thereby allowing PZ to function as a BL-regulated molecular switch. This PZ protein may provide a new design for future optogenetic tools.

MATERIALS AND METHODS

Construction of Expression Vectors. An optimized ZL gene (opZL) encoding Gly^{113}−Lys^{348} of AUREO1 (^{113}ZL, denoted as ZLC_2S in the previous report[29]), in which Cys^{162} and Cys^{182} were substituted with serine and the codons were optimized for bacterial and mammalian expression, was synthesized (GenScript) and inserted into an expression vector as described previously.[27,28] PdK143-F (5′-ATATACCATGGGCAAGTTTCTGCTGGAATCT-3′) and pET-MGK-R (5′-TTGCCCATGGTATATCTCCTTC-3′), PdA180-F (5′-TATACCATGGCCCAGAGCTCTCCGGAAGC-3′) and pET-MAQ-R (5′-CTGGGCCATGGTATATCTCCTTC-3′), and PdP204-F (5′-TATACCATGGGCCCGGACTATAGCCTG-GTG-3′), and pET-MGP-R (5′-CGGGCCCATGGTATATCTC-CTTC-3′) were used as primers with a PrimeSTAR mutagenesis kit (Takara Bio Inc.), for the construction of the expression vectors for Lys^{143}−Lys^{348} (^{143}ZL), Ala^{180}−Lys^{348} (^{180}LOV), and Pro^{204}−Lys^{348} (^{204}LOV), respectively. For the preparation of the recombinant PZs bearing a cysteine residue at the C-terminus (^{113}ZLC, ^{143}ZLC, ^{180}LOVC, and ^{204}LOVC), the expression vector containing opZL was mutated with PdHisCys-F (5′-ACCACTGCTGAGATCCG-GCTGCTAAC-3′) and PdHisCys-R (5′-GATCTCAGCAGTGG-TGGTGGTGGTGG-3′) primers. Sequences of all constructs were confirmed using the Thermo Sequenase Primer Cycle Sequencing Kit (GE Healthcare) with a SQ-5500 DNA sequencer (Hitachi Hitech), and expression vectors of the recombinant PZs were then introduced into BL21(DE3) cells (Invitrogen).

Purification of Recombinant Proteins. Recombinant PZ proteins were prepared as described previously.[27−29] In brief, *Escherichia coli* cells expressing recombinant proteins were harvested by centrifugation and disrupted by sonication. After the cell debris was removed by centrifugation, recombinant proteins were purified twice with a Ni-Sepharose 6 Fast Flow column (GE Healthcare) and a HiTrap Heparin HP column (GE Healthcare), according to the manufacturer's instructions. The recombinant proteins were stored at 4 °C in loading buffer [400 mM NaCl and 20 mM Tris-HCl (pH 7.0)] containing 2 mM DTT, or in PBS buffer [300 mM NaCl and 50 mM sodium phosphate (pH 7.0)] for sulfhydryl modification. Each recombinant protein preparation was denatured by being heated at 95 °C in sodium dodecyl sulfate−polyacrylamide gel electrophoresis (SDS−PAGE) sample buffer for 5 min in the presence of 20 mM DTT and subsequently analyzed by SDS−PAGE. Concentrations of the recombinant proteins were determined from absorbance measurements at 447 nm using an extinction coefficient of 13000 M^{-1} cm^{-1}.[28]

Preparation of Cy-Labeled Recombinant Proteins. Each recombinant protein (40 nmol) bearing a cysteine residue at the C-terminus was incubated in deaerated PBS buffer containing 0.3 mg/mL tris(2-carboxyethyl)phosphine (TCEP) at 25 °C for 10 min. Each sample was reacted with Cy3 or Cy5 maleimide monoreactive dye (GE Healthcare) at 25 °C for 2 h and further incubated overnight at 4 °C. After the removal of unreacted dye with a Ni-Sepharose column (GE Healthcare), the solvent was exchanged to PBS buffer containing 2 mM DTT using a PD-10 column (GE Healthcare), and Cy-labeled proteins were stored at 4 °C until further use. The dye/protein ratios (D/P) were determined by measuring absorbance at 447 nm (protein, ε_{447} = 13000 M^{-1} cm^{-1}) and 553 nm (Cy3, ε_{553} = 150000 M^{-1} cm^{-1}) or 653 nm (Cy5, ε_{653} = 250000 M^{-1} cm^{-1}). The D/P of the Cy-labeled recombinants were 0.12−0.33.

Spectroscopic Measurements. Nonlabeled recombinant proteins were diluted to a concentration of 5 μM in loading buffer containing 1 mM DTT, and Cy-labeled proteins were diluted to 0.4−0.8 μM in PBS buffer containing 1 mM DTT. Ultraviolet−visible (UV−visible) absorption spectra were recorded using a V550 spectrophotometer (JASCO). Spectral changes accompanying regeneration of the dark state (D450 state) were monitored after BL illumination (λ_{max} at 470 nm for 1 min) at 25 °C in the dark. The regeneration curves were obtained from the absorbance at 447 nm. Each absorbance difference curve was fit to a single-exponential term, $\Delta A_{max}(1 - e^{-kt})$, where ΔA_{max} is the maximal absorbance difference and k the rate constant of regeneration. Fluorescence emission spectra were measured at 25 °C with excitation at 450 nm using an F-7000 fluorescence spectrophotometer (Hitachi HiTech).

DLS Measurements. DLS of the protein solutions was measured with a Zetasizer-μV system (Malvern Instruments) in automatic mode at 25 °C, and the z-average molecular sizes expressed as $R_{H(app)}$ in solution were determined using Zetasizer Software (version 6.20) as previously described.[28−30] Briefly, the stock protein solutions were diluted to 40−100 μM with loading buffer containing 1 mM DTT. After removal of the aggregates by centrifugation, light scattering was detected using a solution refractive index of 1.334 and a loading buffer viscosity of 0.9166×10^{-3} Pa s^{-1}. DLS of the recombinant proteins was measured several times in the dark (dark state), and immediately after the termination of BL illumination for 1 min (light state). For measuring DLS in the light−dark state, illuminated samples were incubated for 1 h in the dark after illumination. $R_{H(app)}$ values of samples were plotted versus the concentration, and R_H values were obtained from the extrapolated data at a protein concentration of 0 μM.[28−30] In these experiments, DLS data resulting in a polydispersity index of >0.2 were omitted. Standard

DOI: 10.1021/acs.biochem.5b00320
Biochemistry 2015, 54, 3302−3313

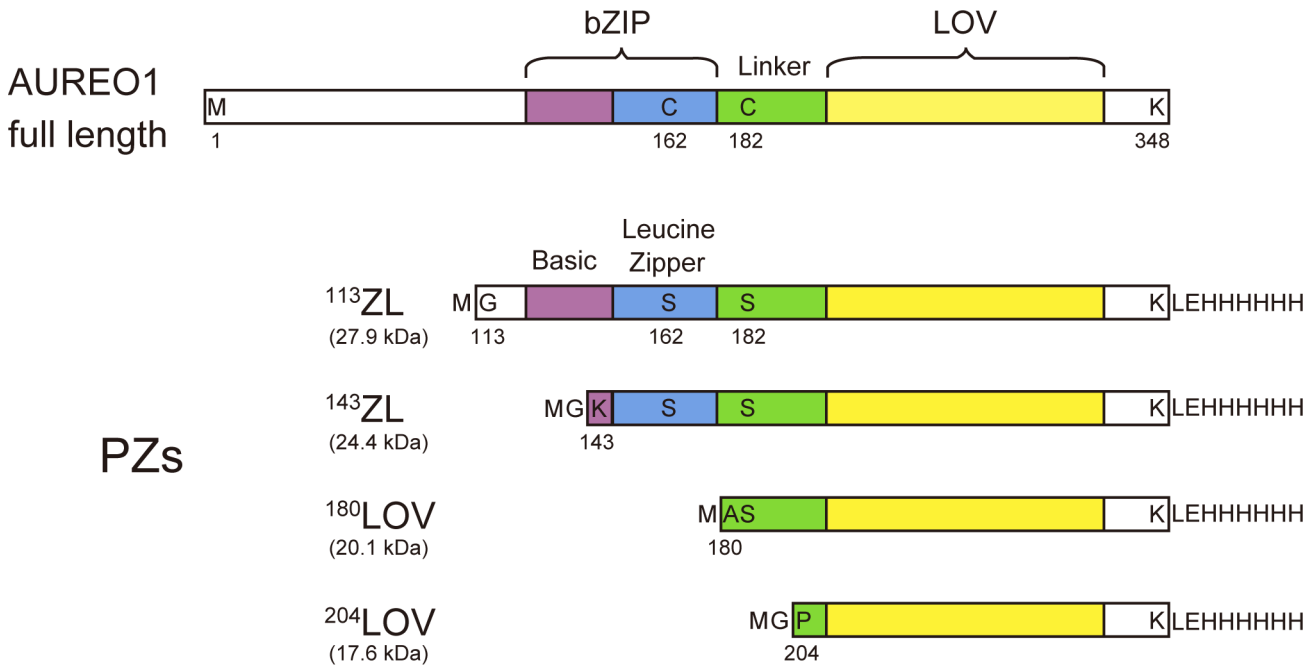

Figure 1. Schematic drawings of the full-length AUREO1 and recombinant PZ proteins, ^{113}ZL, ^{143}ZL, ^{180}LOV, and ^{204}LOV. The amino acid numbering shown is based on full-length AUREO1.

deviations of all $R_{H(app)}$ values obtained from the multiple measurements were less than 0.05 nm.

SEC Measurements. SEC was performed using an AKTA purifier column chromatography system (GE Healthcare) with a Superdex 75 30/10 column (GE Healthcare) using SEC buffer [300 mM NaCl and 20 mM Tris-HCl (pH 7.0)] at 25 ± 1 °C, with a flow rate of 0.5 mL/min.[29] All sample solutions were incubated for 1 h at 25 °C in the dark, and 150 μL aliquots containing 4−100 μM proteins were subjected to analysis (dark state). In the light state, sample solutions were illuminated for 2 min with BL and applied to the column while it was continuously illuminated with a LED. The states of the samples were checked by measuring the absorbance at 390 and 450 nm. For molecular mass calibration of the recombinant proteins, standard spherical proteins in a gel filtration low-molecular weight calibration kit (GE Healthcare) were used as size markers; these included ribonuclease A (13.7 kDa), carbonic anhydrase (29.0 kDa), ovalbumin (43.0 kDa), and conalbumin (75.0 kDa). A column volume of 23.6 mL and a void volume of 6.7 mL were applied. The average molecular weight (MW) was determined using the calibration curve at the peak elution volume. The sample was assumed to be in a monomer−dimer equilibrium, and MW was described by the following equation:

$$\mathrm{MW} = (1 - \alpha)M_\mathrm{m} + \alpha M_\mathrm{d}$$

where M_d is the molecular weight of the dimer calculated by the elution volume of each sample at 100 μM in the light state, M_m is the molecular weight of the monomer (half of M_d), and α is the fraction of dimer as expressed by the following equation:

$$\alpha = \frac{2[\mathrm{dimer}]}{[\mathrm{monomer}]_\mathrm{inj}}$$

α was plotted versus the injected concentration of the monomeric proteins ($[\mathrm{monomer}]_\mathrm{inj}$), and the apparent dissociation constant [$K_{d(app)}$] was estimated from the fitting curve with the following equation:[31−33]

$$K_{d(app)} = \frac{[\mathrm{monomer}]^2}{[\mathrm{dimer}]} = \frac{2(1-\alpha)^2}{\alpha}[\mathrm{monomer}]_\mathrm{inj}$$

$$\alpha = \frac{1}{2}\left\{2 + \frac{K_{d(app)}}{2[\mathrm{monomer}]_\mathrm{inj}} - \sqrt{\left[\frac{K_{d(app)}}{2[\mathrm{monomer}]_\mathrm{inj}}\right]^2 + \frac{2K_{d(app)}}{[\mathrm{monomer}]_\mathrm{inj}}}\right\} \quad (1)$$

FRET Measurements. Fluorescence emission scans were performed using an F-7000 fluorescence spectrophotometer (Hitachi HiTech). Samples were incubated in PBS buffer containing 1 mM DTT and 0.4% (w/v) BSA for 20 min at 25 °C. Samples in the light state were measured immediately after the termination of BL illumination for 1 min. Emission spectra were measured five times from 560 to 700 nm with an excitation wavelength of 550 nm. The extent of FRET was quantified by monitoring the decrease in Cy3 fluorescence at 565 nm. To eliminate the effect of nonlabeled proteins, each FRET spectrum was calculated from the emission spectrum of the solution containing Cy3-PZC and Cy5-PZC minus those containing only Cy3-PZC or only Cy5-PZC, in which the concentrations of Cy-labeled and nonlabeled proteins were adjusted by the addition of nonlabeled samples.

Because the decrease in Cy3 fluorescence (ΔF) by FRET is in proportion to the concentration of Cy3-labeled/Cy5-labeled heterodimer, ΔF is maximized when all proteins in the sample solution form dimers:

$$\Delta F = \Delta f[\mathrm{dimer}_{\mathrm{Cy3-Cy5}}] = \Delta f\beta[\mathrm{dimer}]$$

$$\Delta F_\mathrm{max} = \Delta f\beta\frac{[\mathrm{monomer}]_\mathrm{tot}}{2}$$

where Δf is a constant, β is the fraction of Cy3-labeled/Cy5-labeled heterodimer within all dimer pairs, and ΔF_max is the

DOI: 10.1021/acs.biochem.5b00320
Biochemistry 2015, 54, 3302−3313

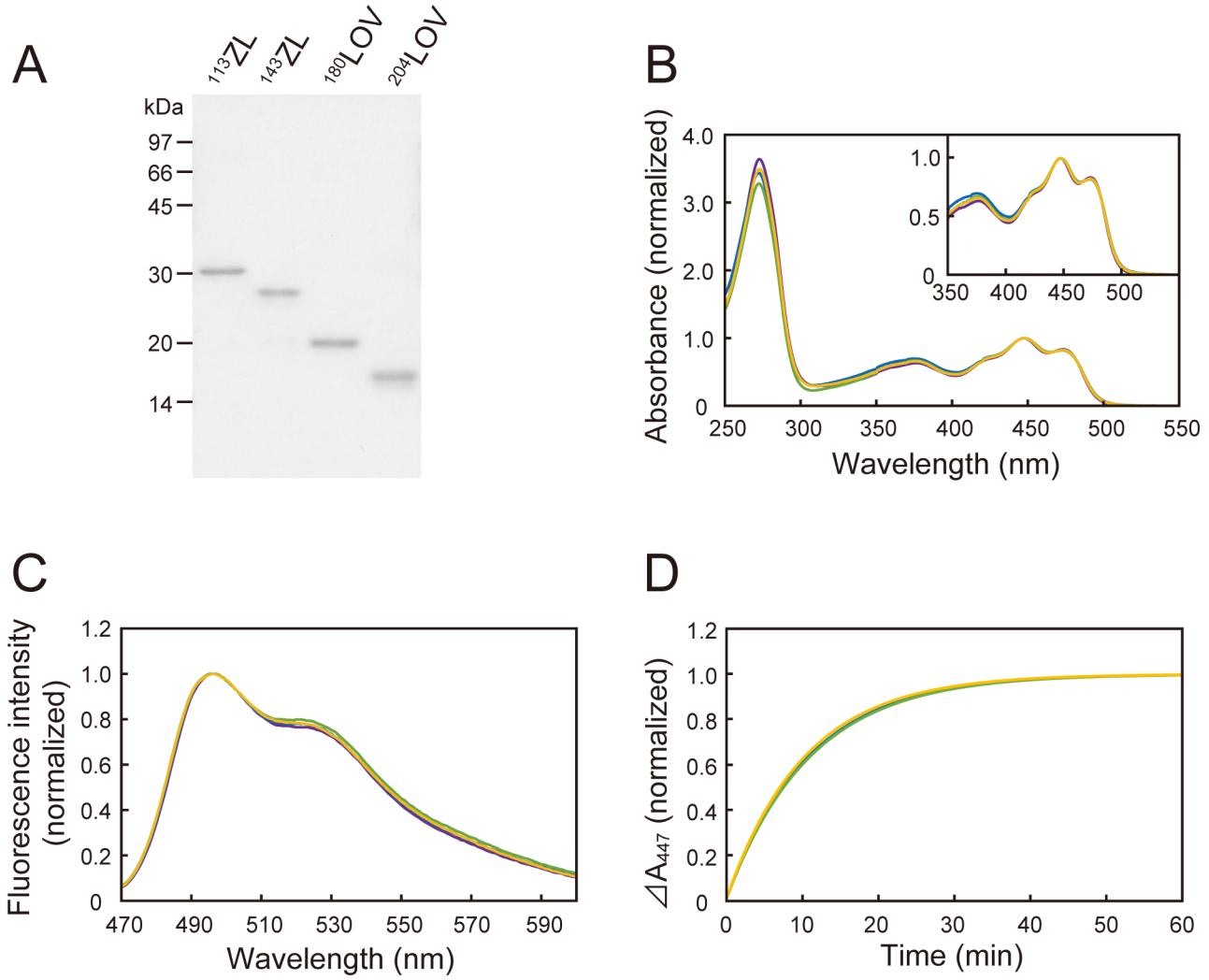

Figure 2. SDS−PAGE and spectroscopic properties of the PZs. (A) Coomassie Brilliant Blue (CBB)-stained SDS−polyacrylamide gel containing ^{113}ZL (lane 1), ^{143}ZL (lane 2), ^{180}LOV (lane 3), and ^{204}LOV (lane 4). UV−visible absorption (B) and fluorescence emission (C) spectra of the recombinant PZs in loading buffer containing 1 mM DTT at 25 °C. Spectra of ^{113}ZL (purple), ^{143}ZL (blue), ^{180}LOV (green), and ^{204}LOV (yellow) are superimposed. The absorption and fluorescent emission spectra were normalized relative to a value of 1.0 at the maximal absorbance (447 nm) and maximal emission (495 nm), respectively. The inset in panel B indicates the enlarged absorption spectra from 350 to 550 nm. (D) Normalized fitting curves of the dark regeneration time course for each PZ using the term $\Delta A_{max}(1 - e^{-kt})$, where ΔA_{max} is the maximal absorption difference and k the rate constant of the reaction. The line types are as in panel B.

maximum of ΔF. Therefore, the dissociation constant (K_d) for the monomer−dimer equilibrium was expressed by the equation

$$K_d = \frac{[\text{monomer}]^2}{[\text{dimer}]} = \frac{2(1 - \Delta F/\Delta F_{max})^2}{\Delta F/\Delta F_{max}}[\text{monomer}]_{tot}$$

If we assume that all combinations of dimer pairs are equally formed, β is constant irrespective of the protein concentration when the fractions of Cy3-labeled, Cy5-labeled, and nonlabeled proteins are constant. In our experiments, the total protein concentration ($[\text{monomer}]_{tot}$) was varied from 20 to 800 nM, and the dissociation constants were obtained from fitting curves with the following equation:

$$\frac{\Delta F}{[\text{monomer}]_{tot}} = \frac{\gamma}{2}\left[2 + \frac{K_d}{2[\text{monomer}]_{tot}} - \sqrt{\left(\frac{K_d}{2[\text{monomer}]_{tot}}\right)^2 + \frac{2K_d}{[\text{monomer}]_{tot}}}\right] \quad (2)$$

$$\gamma = \frac{\Delta f \beta}{2} = \text{constant}$$

RESULTS

Recombinant PZ Proteins. We synthesized an opZL gene encoding AUREO1-ZLC$_2$S (designated as PZ in this work)[28,29] and prepared four different recombinant PZ protein constructs (Figure 1). ^{113}ZL (comprising Gly^{113}−Lys^{348} of AUREO1) contained the basic region/leucine zipper (bZIP) and LOV domains. ^{143}ZL (comprising Gly^{143}−Lys^{348}) contained the leucine zipper (ZIP) and LOV domains but lacked the basic region. ^{180}LOV (comprising Ala^{180}−Lys^{348}) contained the LOV domain and the linker region between the ZIP and LOV domains. ^{204}LOV (comprising Pro^{204}−Lys^{348}) contained only the LOV domain. All the recombinant PZ proteins were fused to a histidine hexamer tag (LEHHHHHH) at the C-terminus.

Figure 2A shows the SDS−PAGE patterns of purified recombinant PZs denatured in the presence of 20 mM dithiothreitol

DOI: 10.1021/acs.biochem.5b00320
Biochemistry 2015, 54, 3302−3313

(DTT). Each recombinant protein appeared as a single band with a molecular weight (MW) of 30 kDa (^{113}ZL), 26 kDa (^{143}ZL), 19 kDa (^{180}LOV), or 16 kDa (^{204}LOV), which is consistent with each MW calculated from the amino acid sequence (27.9, 24.4, 20.1, or 17.6 kDa, respectively).

Absorption and Fluorescence Emission Spectra. The absorption spectra of the recombinant PZs are shown superimposed in Figure 2B. Their absorption spectra in the visible region (Figure 2B, inset) were almost identical to that of AUREO1-ZL, with a λ_{max} at 447 ± 1 nm.[28] Figure 2C shows fluorescence spectra measured with excitation at 450 nm, showing an emission maximum at 495 ± 1 nm with a shoulder at around 530 nm. The absorption spectral changes of recombinant PZs during dark regeneration are shown in Figure S1A–D of the Supporting Information, before illumination (thick solid line), just after BL illumination (dashed line), during dark regeneration (thin line), and 48 min after regeneration (dotted line). The time courses of the regeneration reactions for each of the recombinant PZs monitored at 447 nm were superimposed in Figure 2D. The half-life times ($\tau_{1/2}$) of the reactions were calculated at 7.1–7.6 min, which were comparable with that for the ZL proteins ($\tau_{1/2}$ = 7.2 ± 0.4 min).[28,29] Taken together, these results suggest that the N-terminal truncation of PZ had negligible effects on the π-electron state and photoreactivity of the LOV domain in the recombinant proteins.

DLS Analyses of Recombinant PZs. DLS of the PZ solutions were measured to obtain the proteins' hydrodynamic radii, R_H, from the apparent hydrodynamic radii, $R_{H(app)}$, in the dark (thin solid line), light (dashed line), and light–dark (dotted line) states (Figure 3). The $R_{H(app)}$ values of ^{113}ZL (purple), ^{143}ZL (blue), ^{180}LOV (green), and ^{204}LOV (yellow) depended quasilinearly on their concentration (40–100 μM), as expected from the relationship between interparticle and hydrodynamic interactions, $R_{H(app)} \sim R_H(1 + \theta C)$, where C is the concentration and θ is a constant.[28−30] The R_H values determined by extrapolating the $R_{H(app)}$ to a protein concentration of zero are listed in Table 1. Our previous studies showed that BL induced a 23% increase in R_H (84% increase in volume) primarily because of the dimerization of ^{113}ZL.[29] ^{143}ZL had an R_H of 2.9 nm in the dark state that increased greatly to 3.4 nm following BL illumination. After illumination, the ^{143}ZL solution was kept in the dark for 1 h (the light–dark state), and the R_H was observed to return to 2.9 nm. Like the case for ^{113}ZL, this 17% change in R_H (61% increase in volume) could be explained by a reversible dimerization of ^{143}ZL upon BL illumination. In contrast, ^{180}LOV had an R_H of 2.8 nm in the dark state that increased slightly to 2.9 nm upon BL illumination, and ^{204}LOV showed no R_H change as reported previously.[28] The deletion of the leucine zipper region decreased R_H changes between the dark and light states in the concentration range of 40–100 μM.

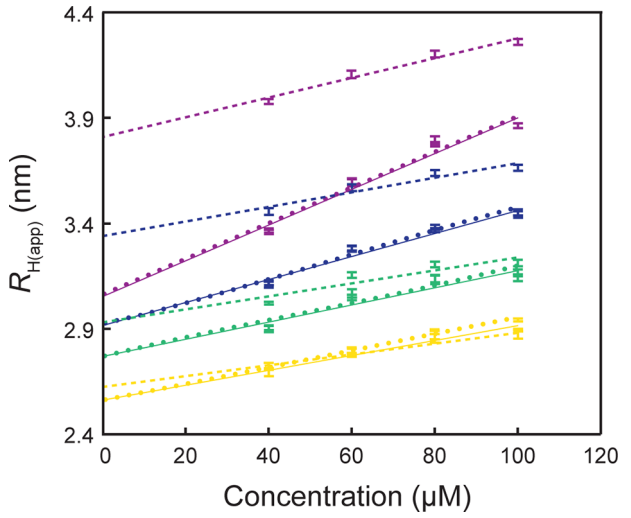

Figure 3. DLS measurements of the PZs. Dependencies of $R_{H(app)}$ on the concentrations of ^{113}ZL (purple), ^{143}ZL (blue), ^{180}LOV (green), and ^{204}LOV (yellow) are superimposed. The regression lines for the dark (thin solid lines), the light (dashed lines), and light–dark (dotted lines) states are shown.

Table 1. R_H Values Estimated from DLS Analyses

	R_H (nm)			
	dark	light	light–dark	volume rate, light/dark
^{113}ZL	3.1	3.8	3.1	1.8
^{143}ZL	2.9	3.4	2.9	1.6
^{180}LOV	2.8	2.9	2.8	1.1
^{204}LOV	2.6	2.6	2.6	1.0

SEC Measurements of Recombinant PZs. To clarify the oligomeric structures at low concentrations, we conducted SEC analyses of the recombinant PZs at 4 μM. Panels A–D of Figure 4 show the elution profiles of ^{113}ZL, ^{143}ZL, ^{180}LOV, and ^{204}LOV, respectively, in the dark state (black lines). The MWs estimated from the calibration line were 39 kDa for ^{113}ZL, 36 kDa for ^{143}ZL, 27 kDa for ^{180}LOV, and 21 kDa for ^{204}LOV. The MWs estimated from the elution peaks of the monomeric PZs were slightly larger than those calculated from the amino acid sequence (28, 24, 20, and 18 kDa, respectively), probably because of their nonspherical shape.[29] In the light state (red lines), the elution peaks shifted to higher molecular weights (62, 61, 49, and 36 kDa). The estimated MWs of each PZ in the light state were 1.6–1.8 times larger than those in the dark state and are comparable with the MWs of the dimeric forms calculated from their amino acid sequences. The elution peaks of the PZs returned to their initial positions in the light–dark state (dotted black lines). These data suggest that like ZLC_2S, the truncated PZs underwent reversible dimerization upon illumination at a concentration of 4 μM, although no large changes in R_H were detected for ^{180}LOV or ^{204}LOV in our DLS studies at protein concentrations of 40–100 μM.

Quantitation of Monomer–Dimer Equilibria in the Dark State by SEC Analyses. To quantify the monomer–dimer equilibria, we investigated the concentration dependencies of the SEC profiles for each of the recombinant PZs. Panels A–D of Figure 5 show the elution profiles of recombinant PZs at 4–100 μM in the dark state (black lines) and the light state (red lines). The elution volumes of all PZs in the light state showed weak dependencies on concentration, suggesting that recombinant PZs in the light state predominantly exist as dimers at these concentrations, and the dissociation constants (K_d) in the light state appeared to be <2 μM. In contrast, the elution volumes in the dark state showed strong dependencies on protein concentration, particularly the peak elution volumes of ^{180}LOV and ^{204}LOV, as these shifted toward those of the light states at high protein concentrations. The dimeric fractions (α) estimated from the peak elution volumes were plotted against the protein concentrations applied to SEC analyses (Figure 5E). If we assums that the elution profiles reflect the equilibria of the injected samples, the apparent dissociation constant [$K_{d(app)}$] was

DOI: 10.1021/acs.biochem.5b00320
Biochemistry 2015, 54, 3302–3313

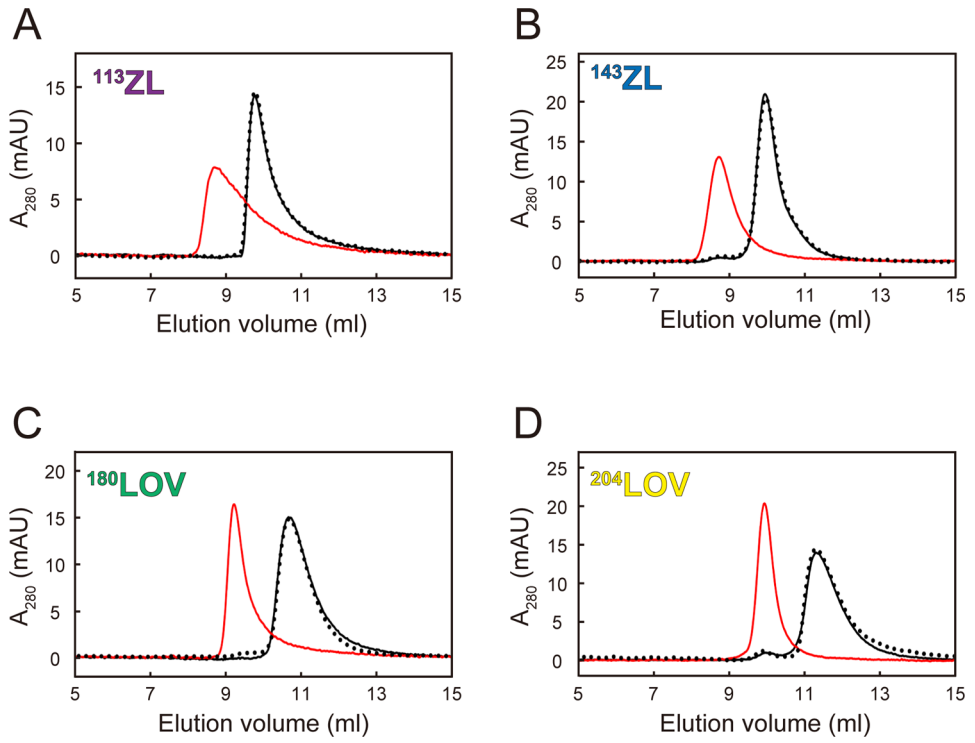

Figure 4. Elution profiles of PZs in SEC buffer monitored by their absorbance at 280 nm. Elution profiles of (A) ^{113}ZL, (B) ^{143}ZL, (C) ^{180}LOV, and (D) ^{204}LOV in the dark state (black lines), the light state (red lines), and the light−dark state (black dotted lines).

estimated from fitting to eq 1. The injected samples were diluted during the chromatographic process; thus, the calculated $K_{d(app)}$ actually provides the upper limit of the K_d.[31−33] The $K_{d(app)}$ values of the recombinant PZs are listed in Table 2. The $K_{d(app)}$ values of ^{113}ZL and ^{143}ZL in the dark state from our SEC analyses were 131 and 91 μM, respectively. The small difference in $K_{d(app)}$ between each ZL can be attributed to the repulsive interactions of charged residues in the basic region.[34,35] The $K_{d(app)}$ values of ^{180}LOV and ^{204}LOV (26 ± 4 and 35 ± 6 μM, respectively) were approximately one-fifth of that for ^{113}ZL, indicating that truncation of the leucine zipper region strongly induced dimer formation. These data suggest that ZLs and LOVs predominantly exist as monomers and dimers, respectively, at protein concentrations of >40 μM, which is consistent with our DLS data showing that N-terminal truncation of PZ reduces the changes in R_H upon BL illumination at concentrations of 40−100 μM.

Cy-Labeled Recombinant PZs. Recombinant PZCs bearing a cysteine residue at the C-terminus (^{113}ZLC, ^{143}ZLC, ^{180}LOVC, and ^{204}LOVC) were prepared and labeled with Cy3 or Cy5. The SDS−PAGE patterns of purified recombinant PZCs were similar to those of the PZs (Figure 6A). The absorption and fluorescence spectra of the nonlabeled PZCs (panels B and C of Figure 6, respectively) were almost identical to those of the PZs. The spectral changes of PZCs (Figure S2A−D of the Supporting Information) and Cy-labeled PZCs (Figure 6D,E and Figure S3A−F of the Supporting Information) during dark regeneration, before illumination (thick solid lines) and just after BL illumination (dashed lines), during dark regeneration (thin lines), and 48 min after regeneration (dotted lines) were measured at 25 °C. The regeneration time courses of ^{113}ZL series (^{113}ZL, ^{113}ZLC, Cy3-^{113}ZLC, and Cy5-^{113}ZLC) monitored at 447 nm were superimposed in Figure 6F, while those of the other series were superimposed in Figure S4A−C of the Supporting Information. The half-life time ($\tau_{1/2}$) of each reaction was calculated at 7.0−7.7 min, which is a range comparable with those of the PZs. These data suggest that the additional cysteine residue and labeling with a Cy fluorophore at the C-terminus had negligible effects on the π-electron state and photoreactivity of the LOV domain in the PZs.

Quantitation of the Monomer−Dimer Equilibria in the Light State by FRET Analyses. Cy3-labeled PZCs (Cy3-PZCs) and Cy5-labeled PZCs (Cy5-PZCs) were used to investigate the monomer−dimer equilibria using FRET. Given that the D/P of our Cy-PZCs were between 0.12 and 0.33, each FRET spectrum was calculated from the emission spectrum of a Cy3-PZC/Cy5-PZC mixed solution minus that for each of the Cy3-PZC and Cy5-PZC solutions alone, to eliminate the effects of nonlabeled PZCs in addition to that of Cy3-PZC/Cy3-PZC and Cy5-PZC/Cy5-PZC homodimers. In the dark state, only slight FRET signals were detected even at a protein concentration of 800 nM [the upper limit of $\Delta F/\Delta F_{max}$ appeared to be <0.2 (data not shown)], and the K_d values of the PZs were estimated to be >2 μM. In the light state, however, incremental increases in the protein concentration resulted in decreasing Cy3 fluorescence around 565 nm and increasing Cy5 fluorescence around 663 nm in a concentration-dependent manner. Panels A−D of Figure 7 show the concentration dependencies of FRET spectra in the light state at 20−800 nM with a fixed ratio of Cy3-PZCs, Cy5-PZCs, and nonlabeled PZCs. The Cy3 fluorescence quenching by FRET ($\Delta F/\Delta F_{max}$) was plotted as a function of total protein concentration (Figure 7E). The K_d values for each PZ estimated from fitting the data to eq 2 are summarized in Table 3. The K_d values for ^{113}ZL and ^{143}ZL in the light state were estimated to be 0.12−0.16 μM, whereas those for ^{180}LOV and ^{204}LOV were 0.59 and 0.55 μM, respectively. Truncation of the ZIP region shifted the monomer−dimer equilibria of the PZs toward the monomeric form, suggesting that the ZIP domain stabilizes the dimeric form in the light state.

DOI: 10.1021/acs.biochem.5b00320
Biochemistry 2015, 54, 3302−3313

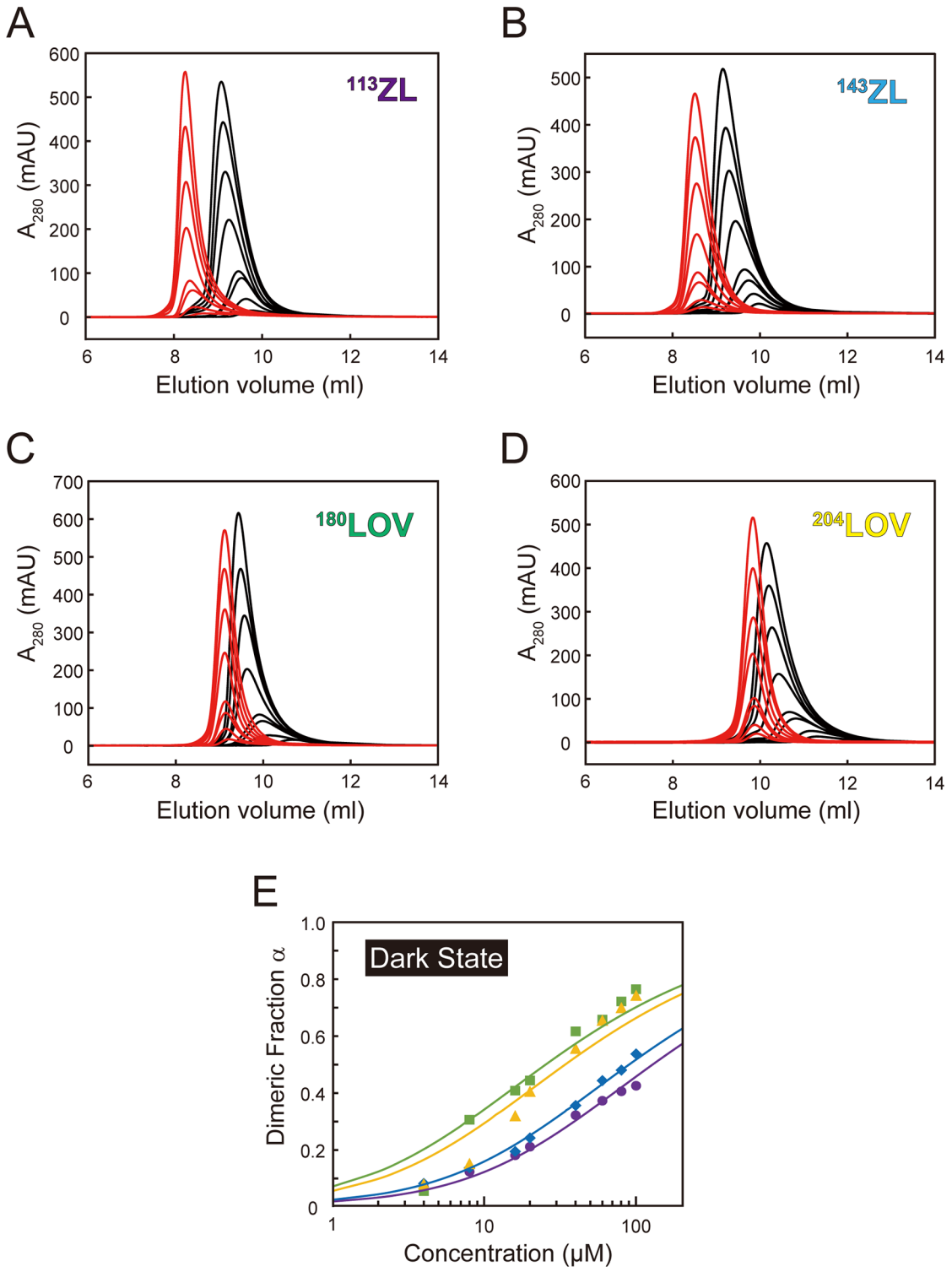

Figure 5. Concentration dependencies of elution profiles of the PZs. Elution profiles of (A) ^{113}ZL, (B) ^{143}ZL, (C) ^{180}LOV, and (D) ^{204}LOV in the dark state (black lines) and the light state (red lines). The injected concentrations of the PZs were 100, 80, 60, 40, 20, 16, 8, and 4 μM (from the highest to the lowest peak, respectively). (E) Dependencies of the dimeric fraction (α) in the dark (filled symbols and fitted lines) on the injected concentrations of ^{113}ZL (purple), ^{143}ZL (blue), ^{180}LOV (green), and ^{204}LOV (yellow).

DISCUSSION

In this study, we performed quantitative analyses of the monomer−dimer equilibria of truncated PZs in the dark and light states. DLS and SEC data showed that all monomeric PZs dimerized upon BL illumination. The K_d values for the dimers of the various bZIP proteins were estimated to be 10^{-8} to 10^{-6} M at 25 °C,[34−36] and those determined in this study for ^{113}ZL (0.12 μM) and ^{143}ZL (0.16 μM) in the light states were within this range. ^{180}LOV and ^{204}LOV in the light states had higher K_d values (0.59 and 0.55 μM, respectively), which were smaller than that for the Vivid (2−10 μM) homodimer in the light state.[16] This is consistent with a luciferase reporter assay indicating that

DOI: 10.1021/acs.biochem.5b00320
Biochemistry 2015, 54, 3302−3313

Table 2. Apparent Dissociation Constants [$K_{d(app)}$] for Each PZ Estimated from SEC Analyses

	$K_{d(app)}$ (μM)	
	dark	light
^{113}ZL	131 ± 6	<2.0
^{143}ZL	91 ± 3	
^{180}LOV	26 ± 4	
^{204}LOV	35 ± 6	

BL-induced dimerization of ^{204}LOV resulted in transcription activity higher than that of Vivid.[23] Our results strongly suggest that the ZIP domain, but not the linker region between ZIP and LOV, contributes to stabilization of the PZ dimer in the light state.

The monomer−dimer equilibria of PZs in the dark state were investigated by comparing SEC profiles. The presence of monomer−dimer equilibria of LOVs in the dark state is consistent with our previous SEC and TG studies, although the concentration range tested was different.[27,28] SEC profiles of a sample in equilibrium depend largely on the experimental conditions, buffer components and temperature, column volume, flow rate, etc.,[37,38] which may cause a wide distribution of K_d values estimated from each SEC experiment. The $K_{d(app)}$ values

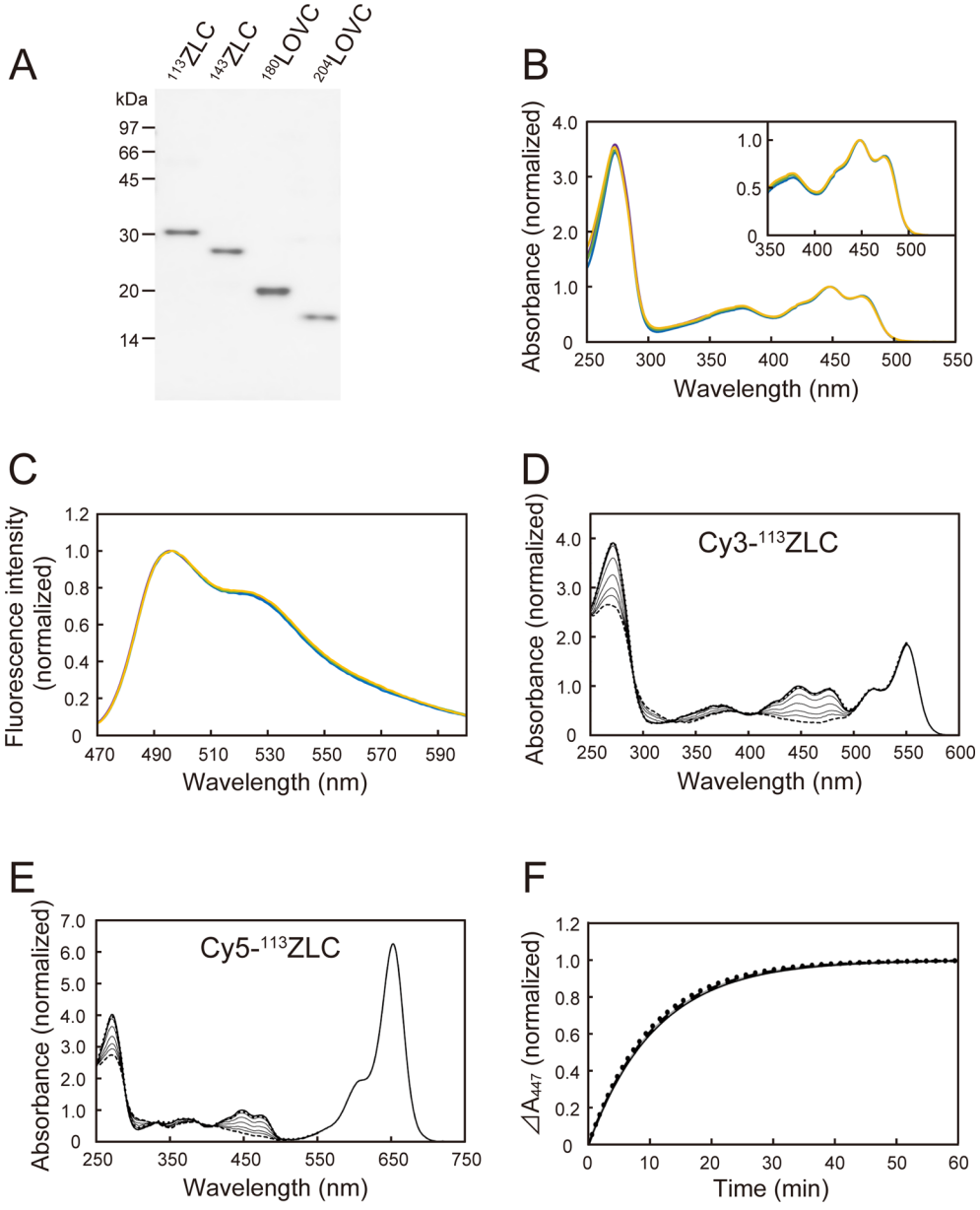

Figure 6. SDS−PAGE and spectroscopic properties of PZCs. (A) CBB-stained SDS−polyacrylamide gel of ^{113}ZLC (lane 1), ^{143}ZLC (lane 2), ^{180}LOVC (lane 3), and ^{204}LOVC (lane 4). UV−visible absorption (B) and fluorescence emission (C) spectra of the recombinant PZCs in loading buffer containing 1 mM DTT at 25 °C. Spectra of ^{113}ZLC (purple), ^{143}ZLC (blue), ^{180}LOVC (green), and ^{204}LOVC (yellow) are superimposed. The absorption and fluorescent emission spectra were normalized relative to a value of 1.0 at the maximal absorbance (447 nm) and maximal emission (495 nm), respectively. The inset indicates the enlarged absorption spectra from 350 to 550 nm. Spectral changes during dark regeneration of D450 from S390 for (D) Cy3-^{113}ZLC and (E) Cy5-^{113}ZLC at 25 °C. The spectra were measured at the initial dark state (solid line) and immediately (dashed line), 2, 4, 8, 16, or 32 min (thin solid lines), or 48 min (thick dotted line) after termination of BL illumination. Normalized fitting curves of the dark regeneration are shown for ^{113}ZL (gray line), ^{113}ZLC (black thin line), Cy3-^{113}ZLC (black dashed line), and Cy5-^{113}ZLC (black dotted line) using the term $\Delta A_{max}(1 - e^{-kt})$ where ΔA_{max} is the maximal absorption difference and k the rate constant of the reaction.

DOI: 10.1021/acs.biochem.5b00320
Biochemistry 2015, 54, 3302−3313

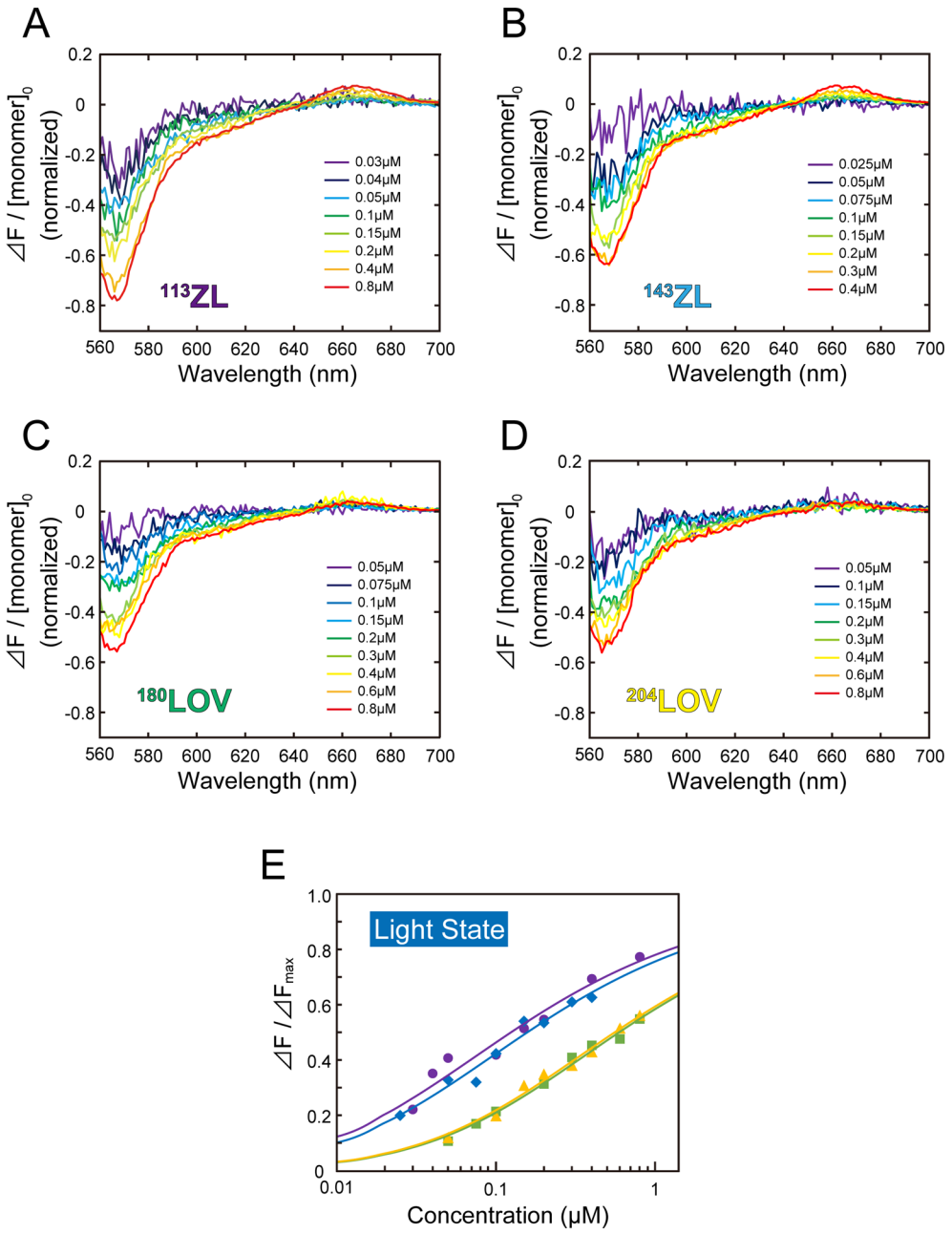

Figure 7. FRET spectra of (A) ^{113}ZL, (B) ^{143}ZL, (C) ^{180}LOV, and (D) ^{204}LOV in the light state at 20−800 nM. Each FRET spectrum was calculated from the emission spectrum of the solution containing a mixture of Cy3-PZC and Cy5-PZC minus those containing only Cy3-PZC and only Cy5-PZC. The decrease in Cy3 fluorescence at 565 nm and the concomitant increase in Cy5 fluorescence at 663 nm by FRET were observed to occur in a concentration-dependent manner. (E) Concentration dependencies of Cy3 fluorescence quenching by FRET ($\Delta F/\Delta F_{max}$) for ^{113}ZL (purple), ^{143}ZL (blue), ^{180}LOV (green), and ^{204}LOV (yellow).

Table 3. K_d Values of the PZs Estimated from FRET Analyses

	K_d (μM)	
	dark	light
^{113}ZL	>2.0	0.12 ± 0.03
^{143}ZL		0.16 ± 0.04
^{180}LOV		0.59 ± 0.08
^{204}LOV		0.55 ± 0.09

of ZLs and LOVs measured under our experimental conditions appeared to be ∼110 and 30 μM, respectively, suggesting that the ZIP region stabilizes the PZ monomer in the dark state.

Mitra et al. reported that the K_d of LOV comprising Asp^{176}−Lys^{337} of *V. frigida* AUREO1 (*Vf*AUREO1) had an upper limit at ∼4 μM when using analytical ultracentrifugation.[39] This construct possibly has the ability to form an intermolecular disulfide linkage through ^{182}Cys, when the ORP of the solution is high.[29] They proposed a crystal structure of the *Vf*AUREO1 LOV core domain in which helices Jα and A′α are located on the outer side of the hydrophobic β-sheet surface (β-scaffold).[39] It has been suggested that BL-induced unfolding of helices Jα and A′α allows dimerization via the β-scaffold of aureochrome1a-LOV of the diatom *Phaeodactylum tricornutum* (*Pt*AUREO1), although *Pt*AUREO1 LOV is monomeric even at a protein concentration of 3.7 mM in the dark state.[40,41] Similar conformational

DOI: 10.1021/acs.biochem.5b00320
Biochemistry 2015, 54, 3302−3313

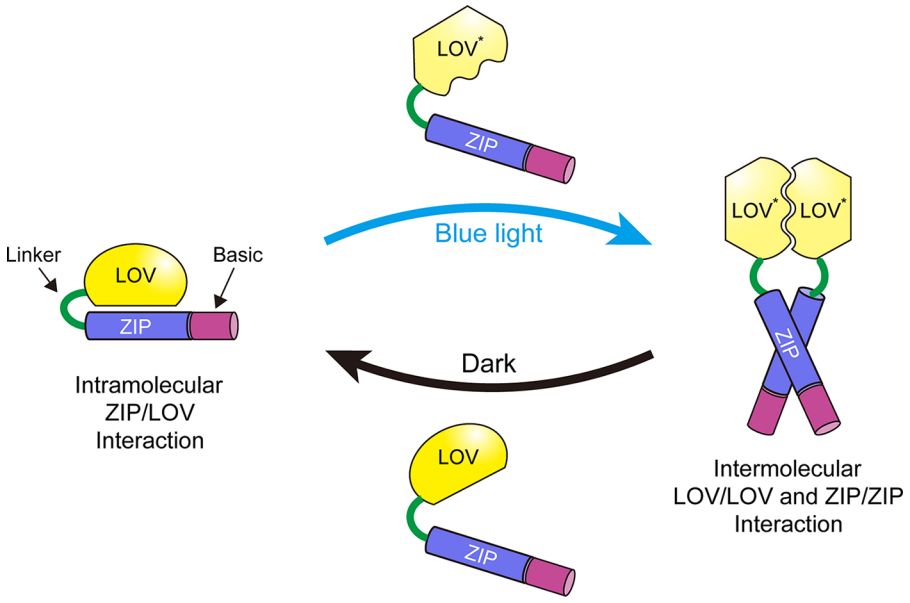

Figure 8. Schematic model of the PZ photoreaction. In the dark state, PZ exists as a monomer with the ZIP region docking onto the LOV domain. BL-induced conformational changes weaken the intramolecular LOV–ZIP interaction, and the bZIP domain then dissociates. In the light state, intermolecular LOV–LOV and ZIP–ZIP interactions stabilize the dimeric form.

features have been suggested for other LOV proteins. phot LOV2 is highly similar to AUREO1-LOV, and its Jα helix docks onto the β-sheet surface.[7,42] In addition, a β-sheet surface of the EL222 LOV domain directly interacts with the HTH domain.[18] Therefore, the ZIP region of PZ possibly interacts with the LOV domain and inhibits LOV/LOV dimerization by shielding the β-scaffold in the dark state.

CD measurements of dimeric $ZLwt_2$ indicated that BL illumination induced α-helical unfolding in the LOV domain and folding in the bZIP and linker regions.[27,28] This may be attributed to the unfolding of the Jα and/or A′α helices in the LOV domain and to the α-helical folding of the bZIP region by coiled-coil interactions. Our data led to the photoreaction scheme of PZ described in Figure 8. In the dark state, the ZIP region shields the dimerization site of the LOV domain, and the intramolecular LOV–ZIP interaction stabilizes the monomeric form. The BL-induced conformational changes in the LOV domain weaken the LOV–ZIP interaction and cause the dissociation of the ZIP domain from the LOV surface. Subsequently, PZ dimerizes via the intermolecular ZIP–ZIP and LOV–LOV interactions. These synergistic interactions between the LOV and bZIP domains stabilize the monomeric form in the dark state and the dimeric form in the light state, and PZ (as well as AUREO1 under reducing conditions) possibly functions as a BL-regulated molecular switch. Because PZ has an effector domain at the N-terminal side of the LOV domain unlike other LOV proteins, PZ may allow the design of optogenetic tools to regulate the activities of domains fused at its N-terminal side.

■ ASSOCIATED CONTENT

Supporting Information

Spectral changes during dark regeneration of D450 from S390 for PZs (Figure S1), PZCs (Figure S2), and Cy-PZCs (Figure S3) at 25 °C and normalized fitting curves of the dark regeneration for PZs, PZCs, and Cy-PZCs (Figure S4). The Supporting Information is available free of charge on the ACS Publications website at DOI: 10.1021/acs.biochem.5b00320.

■ AUTHOR INFORMATION

Corresponding Author

*Department of Earth and Space Science, Graduate School of Science, Osaka University, Toyonaka, Osaka 560-0043, Japan. Telephone: +81-6-6850-5500. Fax: +81-6-6850-5480. E-mail: hisatomi@ess.sci.osaka-u.ac.jp.

Funding

This research was partly supported by a Grant-in-Aid for Scientific Research (C) (26440077 to O.H.) from the Japan Society for the Promotion of Science.

Notes

The authors declare no competing financial interest.

■ ACKNOWLEDGMENTS

We thank Prof. Satoru Nakashima, Dr. Norio Hamada, and Dr. Ryosuke Nakamura (Osaka University) for helpful discussions.

■ ABBREVIATIONS

BL, blue light; LOV, light-oxygen-voltage-sensing; PAS, Per-ARNT-Sim; phot, phototropin; FMN, flavin mononucleotide; HTH, helix–turn–helix; AUREO, aureochrome; bZIP, basic region/leucine zipper; ZIP, leucine zipper; PZ, Photozipper; TG, transient-grating; CD, circular dichroism; DLS, dynamic light scattering; R_H, hydrodynamic radius; $R_{H(app)}$, apparent hydrodynamic radius; λ_{max}, maximal wavelength; SEC, size-exclusion chromatography; MW, molecular weight; ORP, oxidation–redox potential; SDS–PAGE, sodium dodecyl sulfate–polyacrylamide gel electrophoresis; DTT, dithiothreitol; FRET, fluorescence resonance energy transfer; $K_{d(app)}$, apparent dissociation constant; K_d, dissociation constant; CBB, Coomassie Brilliant Blue.

■ REFERENCES

(1) Henry, J. T., and Crosson, S. (2011) Ligand-binding PAS domains in a genomic, cellular, and structural context. *Annu. Rev. Microbiol. 65*, 261–286.

DOI: 10.1021/acs.biochem.5b00320
Biochemistry 2015, 54, 3302–3313

(2) Christie, J. M. (2007) Phototropin blue-light receptors. *Annu. Rev. Plant Biol. 58*, 21−45.
(3) Salomon, M., Christie, J. M., Kneib, E., Lempert, U., and Briggs, W. R. (2000) Photochemical and mutational analysis of the FMN-binding domains of the plant blue light receptor, phototropin. *Biochemistry 39*, 9401−9410.
(4) Swartz, T. E., Corchnoy, S. B., Christie, J. M., Lewis, J. W., Szundi, I., Briggs, W. R., and Bogomolni, R. A. (2001) The photocycle of a flavin-binding domain of the blue light photoreceptor phototropin. *J. Biol. Chem. 276*, 36493−36500.
(5) Iwata, T., Tokutomi, S., and Kandori, H. (2002) Photoreaction of the cysteine S-H group in the LOV2 domain of *Adiantum* phytochrome3. *J. Am. Chem. Soc. 124*, 11840−11841.
(6) Christie, J. M., Swartz, T. E., Bogomolni, R. A., and Briggs, W. R. (2002) Phototropin LOV domains exhibit distinct roles in regulating photoreceptor function. *Plant J. 32*, 205−219.
(7) Harper, S. M., Neil, L. C., and Gardner, K. H. (2003) Structural basis of a phototropin light switch. *Science 301*, 1541−1544.
(8) Harper, S. M., Christie, J. M., and Gardner, K. H. (2004) Disruption of the LOV-Jα helix interaction activates phototropin kinase activity. *Biochemistry 43*, 16184−16192.
(9) Nakasone, Y., Eitoku, T., Matsuoka, D., Tokutomi, S., and Terazima, M. (2007) Dynamics of conformational changes of *Arabidopsis* phototropin 1 LOV2 with the linker domain. *J. Mol. Biol. 367*, 432−442.
(10) Pfeifer, A., Majerus, T., Zikihara, K., Matsuoka, D., Tokutomi, S., Heberle, J., and Kottke, T. (2009) Time-resolved Fourier transform infrared study on photoadduct formation and secondary structural changes within the phototropin LOV domain. *Biophys. J. 96*, 1462−1470.
(11) Yamamoto, A., Iwata, T., Sato, Y., Matsuoka, D., Tokutomi, S., and Kandori, H. (2009) Light signal transduction pathway from flavin chromophore to Jα helix of *Arabidopsis* phototropin1. *Biophys. J. 96*, 2771−2778.
(12) Alexandre, M. T. A., Domratcheva, T., Bonetti, C., van Wilderen, L. J. G. W., van Grondelle, R., Groot, M.-L., Hellingwerf, K. J., and Kennis, J. T. M. (2009) Primary reactions of the LOV2 domain of phototropin studied with ultrafast mid-infrared spectroscopy and quantum chemistry. *Biophys. J. 97*, 227−237.
(13) Buttani, V., Losi, A., Eggert, T., Krauss, U., Jaeger, K. E., Cao, Z., and Gartner, W. (2007) Conformational analysis of the blue-light sensing protein YtvA reveals a competitive interface for LOV-LOV dimerization and interdomain interactions. *Photochem. Photobiol. Sci. 6*, 41−49.
(14) Möglich, A., and Moffat, K. (2007) Structural basis for light-dependent signaling in the dimeric LOV domain of the photosensor YtvA. *J. Mol. Biol. 373*, 112−126.
(15) Zoltowski, B. D., Schwerdtfeger, C., Widom, J., Loros, J. J., Bilwes, A. M., and Crane, B. R. (2007) Conformational Switching in the Fungal Light Sensor Vivid. *Science 316*, 1054−1057.
(16) Zoltowski, B. D., and Crane, B. R. (2008) Light activation of the LOV protein vivid generates a rapidly exchanging dimer. *Biochemistry 47*, 7012−7019.
(17) Vaidya, A. T., Chen, C. H., Dunlap, J. C., Loros, J. J., and Crane, B. R. (2011) Structure of a light-activated LOV protein dimer that regulates transcription. *Sci. Signaling 4*, ra50.
(18) Nash, A. I., McNulty, R., Shillito, M. E., Swartz, T. E., Bogomolni, R. A., Luecke, H., and Gardner, K. H. (2011) Structural basis of photosensitivity in a bacterial light-oxygen-voltage/helix-turn-helix (LOV-HTH) DNA-binding protein. *Proc. Natl. Acad. Sci. U.S.A. 108*, 9449−9454.
(19) Zoltowski, B. D., Motta-Mena, L. B., and Gardner, K. H. (2013) Blue lightinduced dimerization of a bacterial LOV-HTH DNA-binding protein. *Biochemistry 52*, 6653−6661.
(20) Wu, Y. I., Frey, D., Lungu, O. I., Jaehrig, A., Schlichting, I., Kuhlman, B., and Hahn, K. M. (2009) A genetically encoded photoactivatable Rac controls the motility of living cells. *Nature 461*, 104−108.
(21) Wang, X., Chen, X., and Yang, Y. (2012) Spatiotemporal control of gene expression by a light-switchable transgene system. *Nat. Methods 9*, 266−269.
(22) Motta-Mena, L. B., Reade, A., Mallory, M. J., Glantz, S., Weiner, O. D., Lynch, K. W., and Gardner, K. H. (2014) An optogenetic gene expression system with rapid activation and deactivation kinetics. *Nat. Chem. Biol. 10*, 196−202.
(23) Grusch, M., Schelch, K., Riedler, R., Reichhart, E., Differ, C., Berger, W., Ingles-Prieto, A., and Janovjak, H. (2014) Spatio-temporally precise activation of engineered receptor tyrosine kinases by light. *EMBO J. 33*, 1713−1726.
(24) Takahashi, F., Yamagata, D., Ishikawa, M., Fukamatsu, Y., Ogura, Y., Kasahara, M., Kiyosue, T., Kikuyama, M., Wada, M., and Kataoka, H. (2007) AUREOCHROME, a photoreceptor required for photomorphogenesis in stramenopiles. *Proc. Natl. Acad. Sci. U.S.A. 104*, 19625−19630.
(25) Ishikawa, M., Takahashi, F., Nozaki, H., Nagasato, C., Motomura, T., and Kataoka, H. (2009) Distribution and phylogeny of the blue light receptors aureochromes in eukaryotes. *Planta 230*, 543−552.
(26) Ellenberger, T. E., Brandl, C. J., Struhl, K., and Harrison, S. C. (1992) The GCN4 basic region leucine zipper binds DNA as a dimer of uninterrupted α helices: Crystal structure of the protein-DNA complex. *Cell 71*, 1223−1237.
(27) Toyooka, T., Hisatomi, O., Takahashi, F., Kataoka, H., and Terazima, M. (2011) Photoreactions of Aureochrome-1. *Biophys. J. 100*, 2801−2809.
(28) Hisatomi, O., Takeuchi, K., Zikihara, K., Ookubo, Y., Nakatani, Y., Takahashi, F., Tokutomi, S., and Kataoka, H. (2013) Blue light-induced conformational changes in a light-regulated transcription factor, aureochrome-1. *Plant Cell Physiol. 54*, 93−106.
(29) Hisatomi, O., Nakatani, Y., Takeuchi, K., Takahashi, F., and Kataoka, H. (2014) Blue light-induced dimerization of monomeric aureochrome-1 enhances its affinity for the target sequence. *J. Biol. Chem. 289*, 17379−17391.
(30) Takeuchi, K., Nakatani, Y., and Hisatomi, O. (2014) Accuracy of Protein Size Estimates Based on Light Scattering Measurements. *Open J. Biophys. 4*, 83−91 (Article 45372,9; DOI: 10.4236/ojbiphy.2014.42009).
(31) Liu, T., Liu, D., DeRose, E. F., and Mullen, G. P. (1993) Studies of the dimerization and domain structure of gamma delta resolvase. *J. Biol. Chem. 268*, 16309−16315.
(32) Marintchev, A., Robertson, A., Dimitradis, E. K., Prasad, R., Wilson, S. H., and Mullen, G. P. (2000) Domain specific interaction in the XRCC1-DNA polymerase β complex. *Nucleic Acids Res. 28*, 2049−2059.
(33) Szrto, T. H., Rowland, S. L., and King, G. F. (2001) The Dimerization Function of MinC Resides in a Structurally Autonomous C-Terminal Domain. *J. Bacteriol. 183*, 6684−6687.
(34) Dragan, A. I., Frank, L., Liu, Y. Y., Makeyeva, E. N., Crane-Robinson, C., and Privalov, P. L. (2004) Thermodynamic signature of GCN4-bZIP binding to DNA indicates the role of water in discriminating between the AP-1 and ATF/CREB sites. *J. Mol. Biol. 343*, 865−878.
(35) Seldeen, K. L., McDonald, C. B., Deegan, B. J., and Farooq, A. (2008) Thermodynamic analysis of the heterodimerization of leucine zippers of Jun and Fos transcription factors. *Biochem. Biophys. Res. Commun. 375*, 634−638.
(36) Krylov, D., Olive, M., and Vinson, C. (1995) Extending dimerization interfaces: The bZIP basic region can form a coiled coil. *EMBO J. 14*, 5329−5337.
(37) Lou, X., Zhu, Q., Lei, Z., van Dongen, J. L. J., and Meijer, E. W. (2004) Simulation of size exclusion chromatography for characterization of supramolecular complex: A theoretical study. *J. Chromatogr. A 1029*, 67−75.
(38) Yu, C. M., Mun, S., and Wang, N. H. L. (2006) Theoretical analysis of the effects of reversible dimerization in size exclusion chromatography. *J. Chromatogr. A 1132*, 99−108.

DOI: 10.1021/acs.biochem.5b00320
Biochemistry 2015, 54, 3302−3313

(39) Mitra, D., Yang, X., and Moffat, K. (2012) Crystal structures of Aureochrome1 LOV suggest new design strategies for optogenetics. *Structure 20*, 698−706.
(40) Herman, E., Sachse, M., Kroth, P. G., and Kottke, T. (2013) Blue-light-induced unfolding of the Jα helix allows for the dimerization of aureochrome-LOV from the diatom *Phaeodactylum tricornutum*. *Biochemistry 52*, 3094−3101.
(41) Herman, E., and Kottke, T. (2015) Allosterically Regulated Unfolding of the A′α Helix Exposes the Dimerization Site of the Blue-Light-Sensing Aureochrome-LOV Domain. *Biochemistry 54*, 1484−1492.
(42) Halavaty, A. S., and Moffat, K. (2007) N- and C-terminal flanking regions modulate light-induced signal transduction in the LOV2 domain of the blue light sensor phototropin 1 from *Avena sativa*. *Biochemistry 46*, 14001−14009.

DOI: 10.1021/acs.biochem.5b00320
Biochemistry 2015, 54, 3302−3313